# AAV-NRF2 rescues RPE cell function and viability in human IPSC-RPE and mouse models of oxidative stress

Poster number P0508

Patricia Gordon[1], Izabela Klaska[1], Paul Sladen[1], Sarah Wells[1], Arifa Naeem[1], Enrico Mossotto[2], Matthew Roach[1], Tijmen Vermeule[1], Sophia El-Alami[1], Yanai Duran[1], Vivian Lee[1], Monika Pianka[1], Jasmin Patel[1], Bilge Esin Ozturk[1], Sophia Kleine Holthaus[1], Amelia Lane[1] Anastasios Georgiadis*[1]

1. MeiraGTx UK, 34-38 Provost Street, London, N1 7NG, UK
2. MeiraGTx US, 450 East 29th Street, New York, NY 10016, US

## Oxidative stress in age-related macular degeneration (AMD)

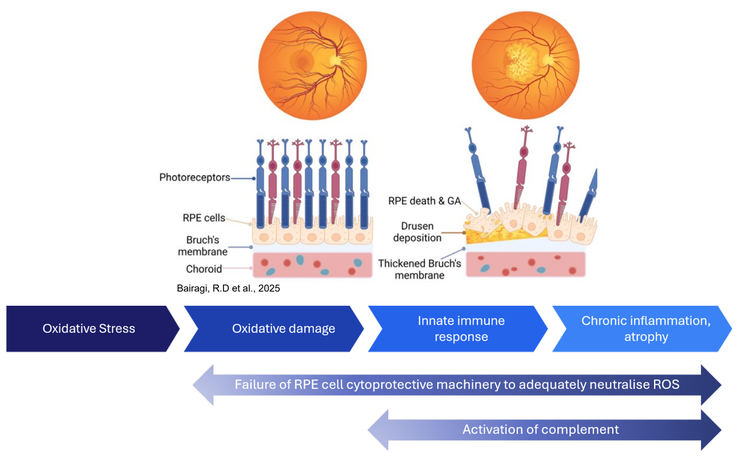


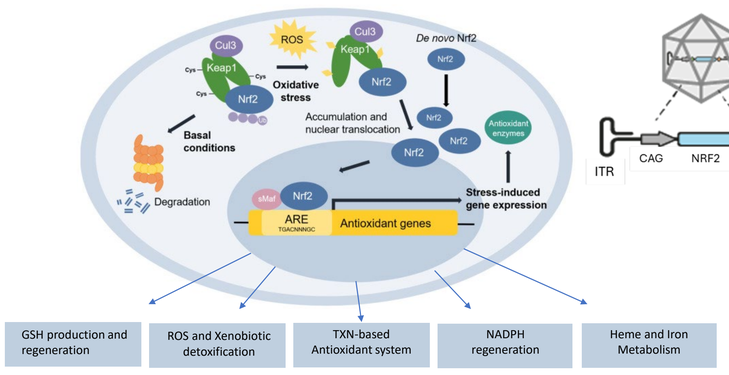


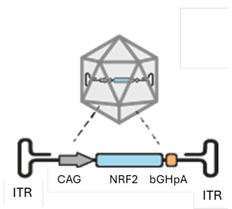


- Age-related macular degeneration (AMD) is a major global cause of irreversible blindness in adults, with nearly 200 million people affected worldwide[1]
- Oxidative stress in the RPE cells is a primary contributor to AMD pathogenesis preceding inflammation and complement pathway activation[2-5]
- NRF2 (nuclear factor erythroid 2-related factor 2) is a master transcription factor regulating the cellular defense against oxidative stress
- Expression constructs comprising NRF2 under the control of a ubiquitous CAG promoter were packaged into AAV capsids with high transduction efficiency in human RPE cells
- *In vitro*, human IPSC-RPE were used to model the impact of oxidative tress on RPE cell function following treatment with tert-butyl hyroperoxide (tBH)
- *In vivo*, the sodium iodate mouse model of RPE atrophy with secondary loss of photoreceptor function was used to model oxidative stress on retinal health
- AAV-NRF2 was able to preserve RPE cell viability and function *in vitro* and preserve both RPE structure and retinal function *in vivo.*
- Novel capsid and promoter combinations are being screened in human IPSC-RPE to improve vector potency and specificity

## *In vitro* - AAV NRF2 preserves RPE cell function in Human IPSC-RPE Oxidative stress model

### Viability

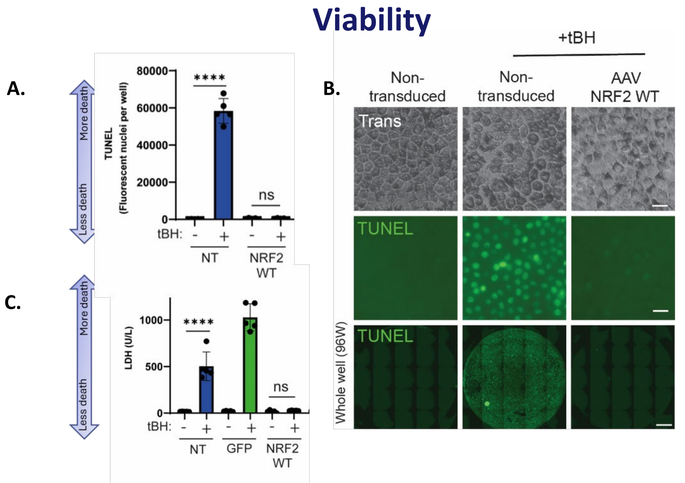


**Fig 1. Quantitative analysis of cell viability in AAV-CAG-NRF2 transduced IPSC RPE following high dose tBH treatment. A.** Quantification of TUNEL staining in AAV-CAG-NRF2 vs non transduced RPE (MOI 1E5 VGs per cell) treated with 1.5mM tBH **B.** Representative images of A. Scale bar = 10µm (top panel) and 1mm (bottom panel showing whole 96 well stitched image). **B. Quantification of** LDH levels in RPE supernatant in non-transduced, control (AAV-CAG-GFP) or AAV-CAG-NRF2 transduced RPE tBH treatment. ***** p<0.0001*. Two-way ANOVA, Sidak's multiple comparison test.

### Barrier function (TER)

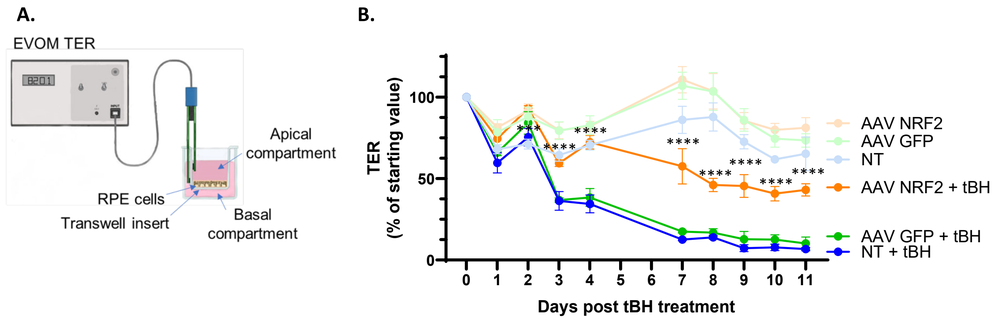


**Fig 2. Quantitative analysis of decline in RPE barrier integrity following tBH induced oxidative stress in non-transduced and AAV CAG-NRF2 transduced IPSC RPE. A.** Schematic of TER set up. IPSC RPE are differentiated on transwells for a 6 weeks. RPE are transduced three weeks prior to tBH treatment (MOI 1E5 VGs per cell) and trans epithelial resistance (TER) is measured before after tBH treatment **B**. TER readings over 11 days following tBH treatment (750uM, bold lines) or no tBH treatment (faded lines). IPSC-RPE were either non transduced, (NT- blue line), Control vector transduced (AAV-GFP, Green line) or transduced with NRF2 (AAV-NRF2, Orange line) *** P=0.0003, ****P <0.0001 vs. NT+ tBH, Two-way ANOVA, Dunnett's multiple comparison test.

### Photoreceptor outer segment (POS) phagocytosis

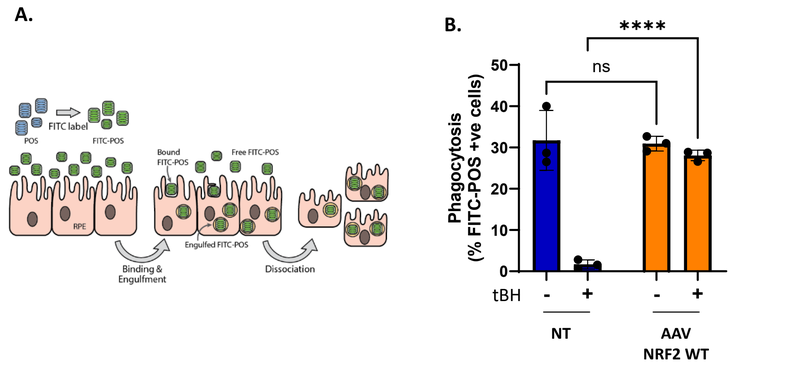


**Fig 3.Phagocytic function in RPE cells following AAV-CAG-NRF2 transduction and tBH treatment.** Schematic of phagocytosis flow cytometry assay. Photoreceptor outer segments (POS) isolated from bovine eyes are labelled with FITC and fed to mature IPSC-RPE cells before dissociation and analysis. IPSC-RPE cells were transduced with AAV-NRF2 (MOI 1E5 VGs per cell) five weeks prior to tBH treatment. After 4 days of tBH treatment (750um), RPE were fed with FITC labelled POS and assayed 5 hours later as single cells. **** p<0.0001 Two-way ANOVA, Sidak's multiple comparison test.

## *In vivo* - AAV NRF2 preserves retinal function in AMD model

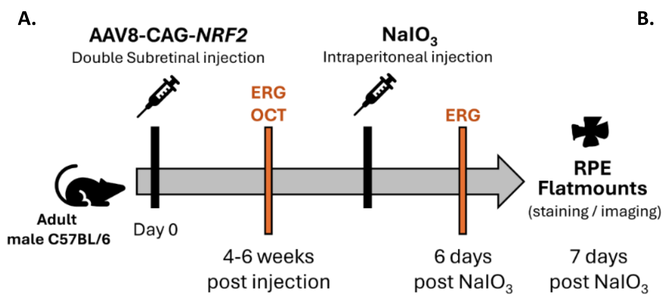


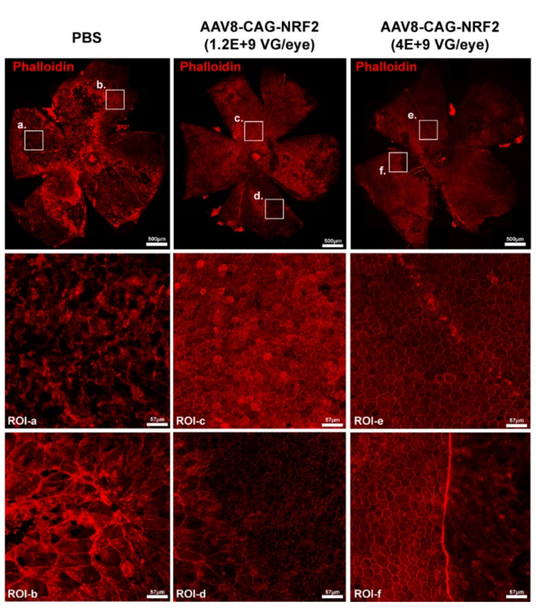


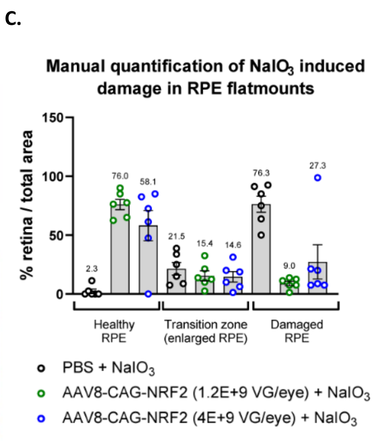


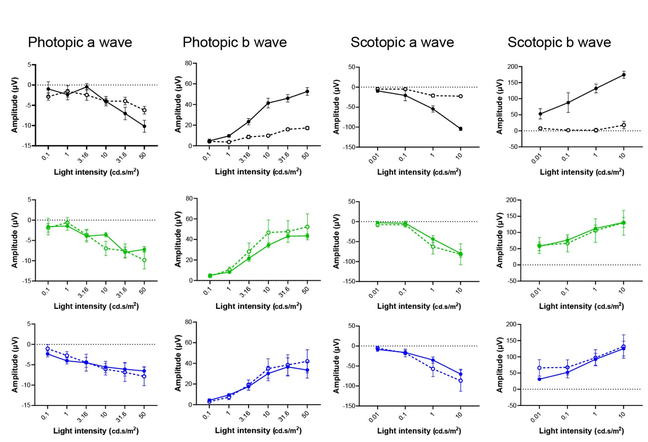


**Fig 4 A. Schematic illustrating experimental protocol steps used.**
Adult male C57BL/6 mice received double subretinal injection of AAV8-CAG-NRF2 at either 1.2E+9 (=3E+11 VG/ml) or 4E+9 VG/eye (=1E+12 VG/ml); control mice received PBS. Four weeks post subretinal injection, whole retina thickness and retinal sensitivity were measured using OCT and ERG, respectively. Sodium iodate (NaIO3) was administered at 20mg/kg body weight by intraperitoneal injection and treatment efficacy of AAV8-CAG-NRF2 was measured 6 days post NaIO3 injection. Following ERG and OCT in vivo assessments mice were culled and RPE flatmounts were stained, imaged and quantified **B. RPE flatmounts stained with phalloidin.** Left panel, PBS treated control group, middle and right panels RPE flatmounts from AAV8-CAG-*NRF2* treated mice at 1.3E+9 VG/eye and 4E+9 VG/eye respectively. .

**C. Semi-quantitative manual assessment of RPE**. For each RPE petal, the approximate percentage area occupied by damaged RPE, the transition zone consisting of enlarged cells, and healthy-looking RPE cells was estimated. Four petals were analysed per sample.

**D. AAV8-CAG-*NRF2* rescues visual sensitivity in mice treated with $NaIO_3$.**
Photopic and scotopic a and b wave amplitudes shown. Top panel: ERG responses in PBS treated control group before (black line) and after (black dotted line) $NaIO_3$, middle panel: ERG responses from mice treated with AAV8-CAG-*NRF2* at 1.3E+9 VG/eye (green line - before $NaIO_3$, green dotted line – after $NaIO_3$), bottom panel: ERG responses from mice treated with AAV8-CAG-*NRF2* at 4E+9 VG/eye (blue line - before $NaIO_3$, green dotted line – after $NaIO_3$). Data from each panel consists of N=6 eyes per treatment group before and after $NaIO_3$ injections.

## AAV-NRF2 vector optimisation

### Engineered Capsids in IPSC-RPE

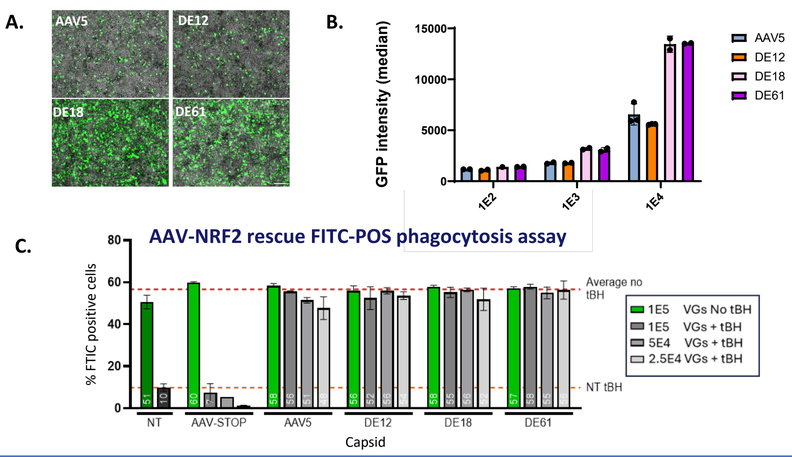


**Fig 5. AAV-NRF2 protects RPE function when delivered in novel engineered capsids with improved RPE infectivity**
**A.** Live imaging showing GFP expression in IPSC-RPE cells transduced with CAG-GFP reporter construct packaged into benchmarking capsids AAV5 and AAV7m8 and novel DE capsids MOI= 1E5 VGs per cell. Scale bar = 100um Flow cytometry analysis of GFP expression in IPSC RPE three weeks post transduction.
**B.** Flow cytometry data from IPSC-RPE cells fed with FITC labelled bovine photoreceptor outer segments following tBH treatment. IPSC-RPE cells were transduced with AAV-NRF2 vectors or control vectors (AAV-STOP) at the indicated MOIs, five weeks prior to tBH treatment. Dashed lines show average % FITC-POS positive cells in the no tBH condition (red) and % FITC-POS positive cells in non-transduced cell tBH treatment. ** *p<0.01* **** *p<0.0001,* Two-way ANOVA and post hoc Tukey's multiple comparison test.

### Promoter activity and specificity

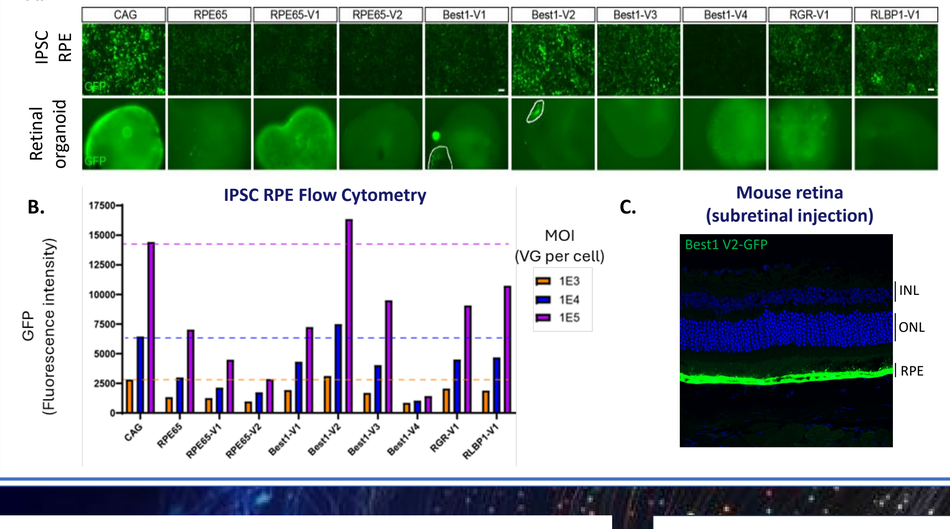


**Fig 6. Novel RPE-specific promoters show improved potency and specificity in IPSC-RPE models and mouse**
**A.** Live fluorescent imaging of RPE (top panel) and retinal organoids (bottom panel) after AAV transduction of GFP driven by CAG or RPE promoters. White circles in organoid panel indicate patches of pigmented RPE cells. **B.** Flow cytometry analysis of GFP fluorescence intensity (right) in RPE transduced at indicated MOIs. Dotted lines indicate expression levels of CAG-GFP at each MOI.
**C**. Mouse retinal cross section following subretinal injection of AAV DE12 Best1 V2 GFP (4E+9 VG/eye). GFP is absent in Inner nuclear layer (INL), photoreceptor layer outer nuclear layer (ONL) and present in the RPE layer. Scale bar = 50µM.

### Conclusions

- NRF2 orchestrates cellular response to oxidative stress, a key mechanistic target in age-related neurodegenerative conditions such as AMD
- *In vitro* **functional assays show complete rescue of RPE function** in AAV-NRF2 treated RPE cells under oxidative stress
- *In vivo* data show that AAV-NRF2 **preserves retinal sensitivity and RPE structure** in a mouse model of oxidative damage
- Vector optimisation can enable RPE-specific expression and functional rescue at lower doses of AAV

**References**
**1. Marchesi, N.**, Capierri, M., Pascale, A., Barbieri, A., Marchesi, N., Capierri, M., Pascale, A., & Barbieri, A. (2024). Different Therapeutic Approaches for Dry and Wet AMD. *International Journal of Molecular Sciences 2024, Vol. 25, 25*(23).
**2. Jadeja, R. N.**, Martin, P. M., Jadeja, R. N., & Martin, P. M. (2021). Oxidative Stress and Inflammation in Retinal Degeneration. *Antioxidants 2021, Vol. 10, 10*(5).
**3. Kushwah, N.**, Bora, K., Maurya, M., Pavlovich, M. C., Chen, J., Kushwah, N., Bora, K., Maurya, M., Pavlovich, M. C., & Chen, J. (2023). Oxidative Stress and Antioxidants in Age-Related Macular Degeneration. *Antioxidants 2023, Vol. 12, 12*(7).
**4. Mimura, T.,** Noma, H., Mimura, T., & Noma, H. (2025). Oxidative Stress in Age-Related Macular Degeneration: From Molecular Mechanisms to Emerging Therapeutic Targets. *Antioxidants 2025, Vol. 14, 14*(10).
**5. Yang, Y. C.**, Chien, Y., Yarmishyn, A. A., Lim, L. Y., Tsai, H. Y., Kuo, W. C., Tsai, P. H., Yang, S. H., Hong, S. I., Chen, S. J., Hwang, D. K., Yang, Y. P., & Chiou, S. H. (2024). Inhibition of oxidative stress-induced epithelial-mesenchymal transition in retinal pigment epithelial cells of age-related macular degeneration model by suppressing ERK activation. *Journal of Advanced Research*, *60*, 141–157.

*Contact: tassos.georgiadis@meiragtx.com*

www.meiragtx.com